
19 Jun 2023

Drug Delivery On Mg-MOF-74: The Effect Of Drug Solubility On Pharmacokinetics

Neila Pederneira

Kyle Newport

Shane Lawson

Ali A. Rownaghi

Missouri University of Science and Technology, rownaghia@mst.edu

et. al. For a complete list of authors, see https://scholarsmine.mst.edu/che_bioeng_facwork/1592

Follow this and additional works at: https://scholarsmine.mst.edu/che_bioeng_facwork

 Part of the [Biochemical and Biomolecular Engineering Commons](#)

Recommended Citation

N. Pederneira et al., "Drug Delivery On Mg-MOF-74: The Effect Of Drug Solubility On Pharmacokinetics," *ACS Applied Bio Materials*, vol. 6, no. 6, pp. 2477 - 2486, American Chemical Society, Jun 2023.

The definitive version is available at <https://doi.org/10.1021/acsabm.3c00275>

This Article - Journal is brought to you for free and open access by Scholars' Mine. It has been accepted for inclusion in Chemical and Biochemical Engineering Faculty Research & Creative Works by an authorized administrator of Scholars' Mine. This work is protected by U. S. Copyright Law. Unauthorized use including reproduction for redistribution requires the permission of the copyright holder. For more information, please contact scholarsmine@mst.edu.

Drug Delivery on Mg-MOF-74: The Effect of Drug Solubility on Pharmacokinetics

Neila Pederneira, Kyle Newport, Shane Lawson, Ali A. Rownaghi, and Fateme Rezaei*

Cite This: *ACS Appl. Bio Mater.* 2023, 6, 2477–2486

Read Online

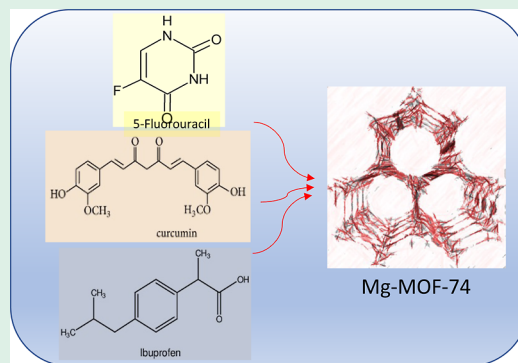
ACCESS |

Metrics & More

Article Recommendations

ABSTRACT: Biocompatible metal–organic frameworks (MOFs) have emerged as potential nanocarriers for drug delivery applications owing to their tunable physicochemical properties. Specifically, Mg-MOF-74 with soluble metal centers has been shown to promote rapid pharmacokinetics for some drugs. In this work, we studied how the solubility of drug impacts the pharmacokinetic release rate and delivery efficiency by impregnating various amounts of ibuprofen, 5-fluorouracil, and curcumin onto Mg-MOF-74. The characterization of the drug-loaded samples via X-ray diffraction (XRD), N₂ physisorption, and Fourier transform infrared (FTIR) confirmed the successful encapsulation of 30, 50, and 80 wt % of the three drugs within the MOF structure. Assessment of the drug delivery performances of the MOF under its various loadings via HPLC tests revealed that the release rate is a direct function of drug solubility and molecular size. Of the three drugs considered under fixed loading condition, the 5-fluorouracil-loaded MOF samples exhibited the highest release rate constants which was attributed to the highest degree of solubility and smallest molecular size of 5-fluorouracil relative to ibuprofen and curcumin. It was also noted that the release kinetics decreases with drug loading, due to a pharmacokinetic shift in release mechanism from singular to binary modes of compound diffusion. The findings of this study highlight the effects of drug's physical and chemical properties on the pharmacokinetic rates from MOF nanocarriers.

KEYWORDS: metal–organic framework, drug delivery, ibuprofen, 5-fluorouracil, curcumin



1. INTRODUCTION

The administration of therapeutic pharmaceutical compounds (i.e., drugs) through orally ingested tablets is one of the most important areas of medicinal science due to its simplicity and ability to deliver nearly any compound. However, tablet-based drug delivery platforms often show bursting of the binder phase, thus administering high concentrations of the therapeutic species which can give rise to health issues including reduced drug efficacy, stomach ulcers, or liver necrosis.^{1–3} Because of such issues, alternative pathways through which drugs can be administered have been developed.

One such notable pathway has been to administer medicinal drugs on nanoporous carrier materials, such as activated carbon, zeolites, and metal–organic frameworks (MOFs).^{4–6} Of these, MOFs have gathered significant momentum as a drug delivery platform due to their high internal surface area—which enables large quantities to be impregnated—as well as on account of their flexible chemical properties. The latter aspect is of significant interest regarding the application of drug delivery, in general, since the ability to vary both the organic ligand and metallic center can be used to enhance the biocompatibility and/or bioavailability. For example, MOFs

with metallic centers such as Zn, Mg, Co, or Ni have been reported as potential drug carriers, all of which are available in the everyday diet.⁷ Hence, the biocompatibilities of these materials should be improved compared to zeolite or activated carbon, in general. Regarding the influence of MOF metallic center on bioavailability and pharmacokinetic release properties, we have shown in our previous works that utilization of Mg-based MOFs enables faster release kinetics of curcuminoids or ibuprofen, on account of the high metal center solubility.⁸ Hence, it is an attractive candidate from the MOF-74 family to use in better understanding various parameters which influence the drug delivery behaviors of MOFs. As another example, Hartleib et al.⁹ loaded ibuprofen onto CD-MOF and demonstrated an uptake of 23–26 wt % of the drug within the CD-MOF. Owing to their adoptable framework for functionalization and fine-tuning, and weak coordination

Received: April 11, 2023

Accepted: May 29, 2023

Published: June 8, 2023

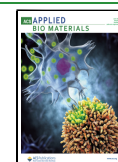
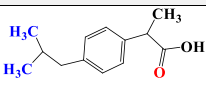
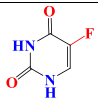
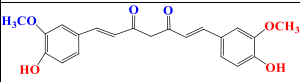


Table 1. Properties of the Three Drugs Investigated in This Work

Drug	Chemical Structure	Solubility in PBS (mg/mL)	Molecular Weight (g/mol)	Degree of Polarity
Ibuprofen		21	206.3	Nonpolar
5-fluorouracil		68	368.4	Polar
Curcumin		0.1	130.1	Moderately polar

bonds, MOFs are promising candidates as nanocarriers for incorporation of various drugs.^{10–14}

Nevertheless, even though MOFs have been well established as drug carriers for the better part of the past decade, many of the fundamental properties which influence the kinetic rate of delivery for MOF/drug systems have yet to be investigated. One such property is the influence of the impregnated drug on the pharmacological release kinetics. This particular property is of high importance to developing MOFs as drug carriers, as the molecular size of the drug as well as its hydrogen bonding and van der Waals interactions with the MOF structure should lend themselves to variable bond strengths. Indeed, a similar phenomenon has been observed in adsorption applications for volatile organic compounds (VOCs), where it is well known that larger molecules will desorb at higher temperatures relative to smaller hydrocarbon species. Given that drug encapsulation onto MOFs is primarily driven by the same type of mechanism—namely, pore filling, followed by condensation on the oriented crystalline surface¹⁵—it stands to reason that the molecular drug size and electrostatic properties would influence the rate of delivery.

However, to our knowledge, this fundamental property has yet to be systematically investigated, so we embarked on a study which targets the relationship between drug solubility in phosphate-buffered saline (PBS), maximal effective loading, and pharmacokinetic rate. Specifically, this study utilized Mg-MOF-74 as a drug delivery platform and varied the loadings of ibuprofen, 5-fluorouracil, and curcumin between 30, 50, and 80 wt % to assess differences in the pharmacokinetic release rates of the MOF@drug composites as a function of drug loading and type with a fixed MOF carrier. Three drugs were selected for this purpose: ibuprofen (anti-inflammatory), curcumin (anti-inflammatory), and 5-fluorouracil (cancer drug). The selection bases for these drugs were based on their solubilities, polarities, and functional moieties which are representative of other commonly administered drugs, as shown in Table 1. For example, ibuprofen is a nonpolar compound with a carboxylic acid functional group whose solubility in PBS is ~21 mg/mL at room temperature.¹⁶ By contrast, 5-fluorouracil, which is more polar than ibuprofen, has a solubility of ~68 mg/mL in PBS at room temperature,¹⁷ whereas the highly lipophilic curcuminoid compounds—which contain diketone and phenolic moieties—have poor solubilities in water-based solutions such as PBS (~0.1 mg/mL at room temperature).¹⁸ Therefore, these drugs can be considered representative of several types of compounds regarding their release from

MOFs, as high-, mid-, and low-solubility species were selected. The various samples were characterized by X-ray diffraction, N₂ physisorption, and Fourier transform infrared spectroscopy (FTIR) before and after drug impregnation to determine the degree of structural retention and to confirm the drug loadings. The drug delivery performances of the various composites were then assessed in PBS solution for 24 h, and the pharmacokinetic rates were calculated using the Higuchi model.^{19–22} Since this study investigates three different drugs, we do anticipate the findings to be relevant to MOF/drug delivery platforms, so the findings herein represent an important fundamental piece of information to the area of MOFs as drug delivery platforms.

2. EXPERIMENTAL SECTION

2.1. Materials. The chemicals used in this project were all purchased from Sigma-Aldrich and used without further modifications. 2,5-Dihydroxyterephthalic acid (DHTA, 98%), Mg(NO₃)₂·6H₂O (99%), *N,N*-dimethylformamide (DMF, ACS), and ethanol (EtOH, ACS) were used for Mg-MOF-74 synthesis; methanol (MeOH, ACS) was used as a solvent for drug impregnation; ibuprofen, 5-fluorouracil, and curcumin were used as drugs; and acetonitrile (ACN, HPLC), distilled water (HPLC), and PBS (pH = 7.4) were used in the HPLC experiments.

2.2. Mg-MOF-74 Synthesis and Drug Impregnation. Mg-MOF-74 was synthesized using a previously reported solvothermal procedure.¹⁵ Briefly, in 45 mL of DMF, both 0.112 g of DHTA and 0.475 g of Mg(NO₃)₂·6H₂O were dissolved with the aid of sonification in a solution containing 3 mL of ethanol and 3 mL of DI water. The solution was then placed inside a 125 °C oven for 21 h. After cooling to room temperature, the liquid was replaced with methanol, followed by washing with methanol for 2 days, with regular decantation and replacement of the solvent during this period. Upon complete wash, the sample was placed in a vacuum oven and heated to 250 °C for 6 h. The samples were then cooled to room temperature.

After synthesis and activation and prior to drug impregnation, the MOF samples were dried overnight under vacuum at 100 °C. Then, the desired amount of ibuprofen, 5-fluorouracil, and curcumin (i.e., 30, 50, and 80 wt %) was incorporated into the MOF structure via the wet-impregnation technique that has been described in detail in previous works.¹⁰ Briefly, the desired amount of the three aforementioned drugs was dissolved in 10 mL of MeOH/0.05 g drug by sonication at room temperature for 15 min until the solution became clear. Then, 0.1 g of Mg-MOF-74 was added to the solution, and the flask was sealed and placed on a magnetic stirring plate and stirred at 200 rpm for 24 h at room temperature. Afterward, the drug-loaded MOF was recovered by rotary evaporation at 70 °C by maintaining the rotation at 10 rpm for about 10 min until the MOF became dry. Then, the dried sample was placed under vacuum at 25

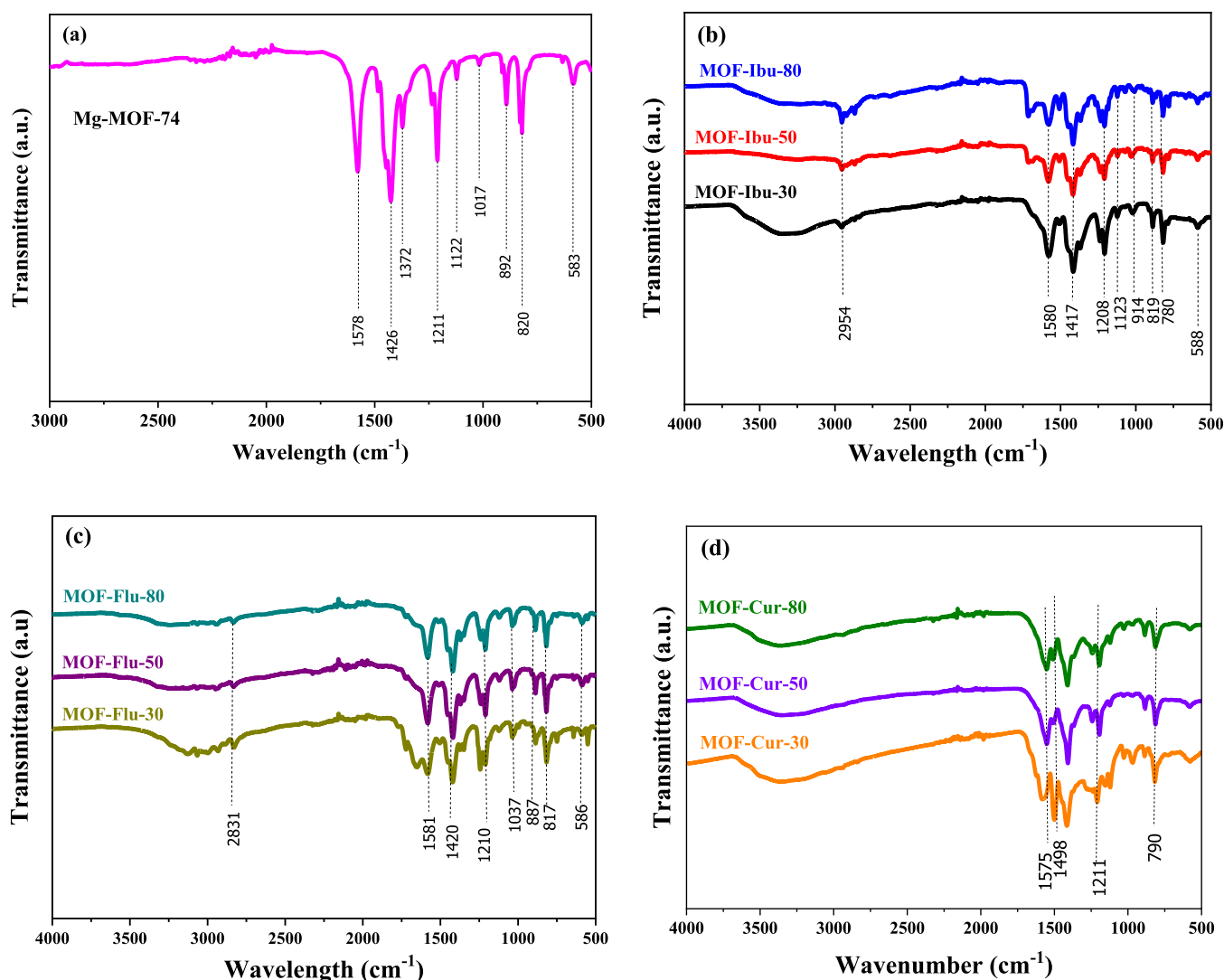


Figure 1. FTIR spectra of (a) bare Mg-MOF-74, (b) ibuprofen-loaded Mg-MOF-74, (c) 5-fluorouracil-loaded Mg-MOF-74, and (d) curcumin-loaded Mg-MOF-74.

°C for 12 h to further remove any moisture and impurities in the material pores prior to the HPLC experiments.

It should be noted here that DMF is poisonous and can lead to medical issues such as cancer formation, liver disease, and kidney failure, so use of DMF for synthesis in an actual medical application is not recommended. However, one can expect the findings in this study to translate across synthetic protocols for Mg-MOF-74, in that they emphasize interactions between the MOF/drug system and are less contingent on the drug/residual solvent interplay. In future works, we will modulate the synthesis to utilize biocompatible solvents such that the relationship between drug type, synthetic chemistry, and pharmacokinetic performance may be better understood. As a first step, however, this work uses the standard DMF Mg-MOF-74 synthesis.

2.3. Drug-Loaded MOF Characterization. The textural properties of the bare MOF and its drug-impregnated analogues were determined via N_2 physisorption analysis at 77 K on a Micromeritics 3Flex gas analyzer. It should be noted here that N_2 physisorption is considered a standard method through which the drug loading efficiency can be approximated, as thermal degradation techniques are generally impractical for drug/MOF composites given that the impregnates decompose at roughly the same temperature as the MOF ligand.⁸ The bare Mg-MOF-74 was degassed before analysis at 110 °C for 6 h on a Micromeritics Smart VacPrep. However, the drug-loaded MOFs were degassed at a lower temperature (100 °C) and

shorter time (1 h) to minimize drug volatilization. The degassing conditions are detailed in our previous works.^{7,23} From the physisorption isotherms, BET surface area, pore volume, and pore size distribution (PSD) of the samples were estimated by the Brunauer–Emmet–Teller (BET) and nonlocal density functional theory (NLDFT) methods, respectively.¹⁵ To determine the crystallographic structure of the samples, X-ray diffraction (XRD) analysis was carried out on a PANalytical XPert multipurpose X-ray diffractometer with a scan step size of 0.02°/step at a rate of 137.2 s/step. Fourier transform infrared (FTIR) equipped with a total reflectance diamond (ATR) was used to assess the samples' functional groups. Prior to XRD and FTIR measurements, all samples were first exposed to PBS at 37 °C for 24 h, then dried under vacuum overnight to assess any changes in crystallinity, and chemical structure arising from PBS exposure.

2.4. Drug Release Experiments. The drug delivery experiments with ibuprofen, fluorouracil, and curcumin were performed via HPLC analysis using an Agilent 1260 Infinity II following the established procedures described in our previous works.^{8,15,24,25} Prior to the start of the experiments, dilute hydrofluoric acid was used to clean all PTFE bottles followed by drying under vacuum for 12 h at 50 °C to make sure any contaminants were removed. The experiments were conducted for a period of 24 h in PBS solution which was first heated to 37 °C to simulate human body fluid and temperature conditions. In each run, 0.05 g of drug-impregnated MOF was diluted in 100 mL of

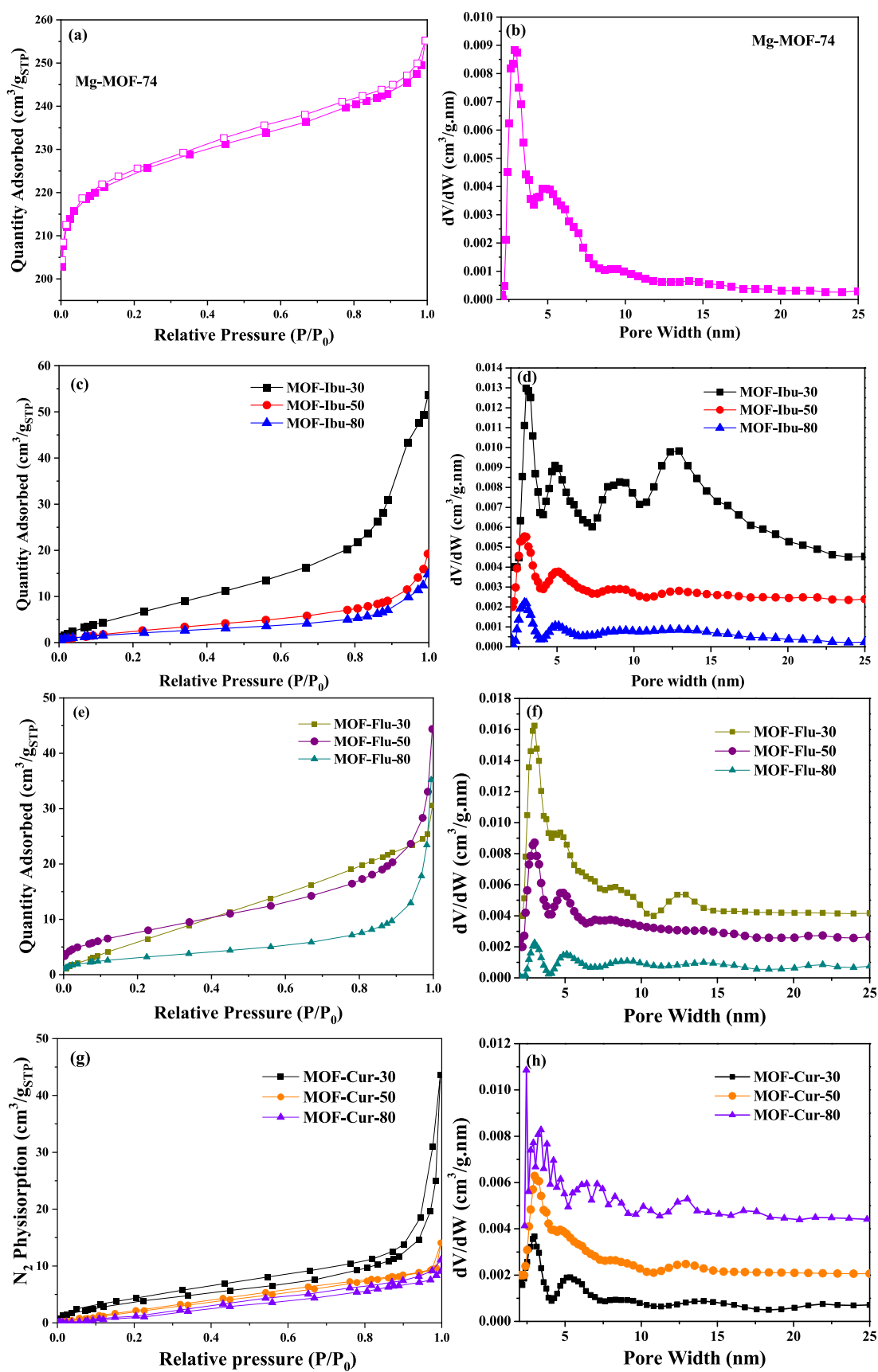


Figure 2. N_2 physisorption isotherms and PSD profiles, with an offset of 0.002, for (a,b) bare Mg-MOF-74, (c,d) ibuprofen-loaded Mg-MOF-74, (e,f) 5-fluorouracil-loaded Mg-MO-74, and (g,h) curcumin-loaded Mg-MOF-74.

PBS for 1–10 h, and samples were collected and placed inside a HPLC vial for analysis every hour for 1–10 h and then again at 24 h. The HPLC system operated with a C₁₈ column of 4.6 × 100 nm dimensions. The HPLC analysis on the collected samples was performed using a previously reported technique,²⁶ and the normalized release kinetics were fitted using the Higuchi approach.^{27,28} To have a valid comparison, all experimental parameters were kept identical across all runs. The Higuchi is a standard model for quantification of drug release from nanocarriers based on the assumption that the effects of drug solubility and diffusivity, solvent diffusivity, and nanocarrier tortuosity are negligible.^{8,29} These assumptions are typically held valid for most porous drug carriers and, therefore, we applied the Higuchi technique in this study with a reasonable degree of confidence, as shown in eq 1.^{15,27}

$$c = kt^{1/2} \quad (1)$$

where c is the drug concentration (%), k is the release rate constant ($h^{-1/2}$), and t is the time of release (h). The drug release data were fitted with the above equation by maximizing the R^2 to estimate the k values for all the materials.

3. RESULTS AND DISCUSSION

3.1. Drug-Loaded MOF Characterization. To confirm the impregnation of drugs into MOF-74, we obtained the FTIR spectra of the drug-loaded samples along with the bare material, as shown in Figure 1. As evident from Figure 1a, the vibrational transmittance bands at 1578, 1426, 1372, 1211, 1122, 1017, 892, 820, and 586 cm^{-1} are characteristics of Mg-MOF-74, which correspond to C=C/C=O conjugation, –OH, C–O, C–O, secondary alcohol C–O, anhydride, C=C, and C=C bonding, respectively.⁸ After impregnating ibuprofen, 5-fluorouracil, and curcumin, several new vibrational bands in the spectra of the drug-loaded sample were observed, as evident from Figure 1b–d, which were consistent with the chemical bands present in these drugs. Specifically, the spectra of ibuprofen-loaded samples displayed additional vibrational bands at 2954, 914, and 780 cm^{-1} , which were related to C–H (aryl), *trans*-CH, and C–H (alkene), respectively, which were all preset within the ibuprofen structure (Figure 1b).²⁸ Meanwhile, the 5-fluorouracil-loaded samples (Figure 1c) displayed a new band at 2831 cm^{-1} , which corresponds to the C–H (methyl) within the 5-fluorouracil structure. As for the curcumin-loaded samples, new transmittance bands related to the vibrational modes of C–O–C, C–H (methyl), and C–H (aryl) were observed at 1023, 2800, and 2900 cm^{-1} , respectively, which can be found in the structure of this drug (Figure 1c).^{8,30,31} Otherwise, it should be noted here that the impregnated MOFs all retained their vibrational bands from the parent MOF, indicating that impregnation of the drugs did not produce any discernible changes in chemical structure for the parent carrier. On this basis, the drugs were concluded to be truly impregnated rather than tethered to the MOF surface, which is important in ensuring that the appropriate therapeutic compound is being administered rather than some partially conjugated analogue.

The N₂ physisorption isotherms and NLDFT PSD profiles are presented in Figure 2. These measurements were conducted to determine any changes to the surface area and porosity of the MOF before and after ibuprofen, 5-fluorouracil, and curcumin incorporation with different loadings. First looking at the results of Mg-MOF-74, the material displayed its typical type I–IV physisorption isotherm (Figure 2a), which agrees with its known micro/mesoporous structure.³² This is further supported by its PSD profile (Figure 2b), which

displayed two prominent pore sizes centered at 2 and 5 nm. Such a hierarchical pore network for the bare MOF is an advantage from drug delivery point of view, as it allows impregnation of substantial amounts of drug within the nanocarrier without blocking the diffusive paths during subsequent release. Regarding the drug-loaded samples, it should first be noted that both ibuprofen (Figure 2c,d) and 5-fluorouracil (Figure 2e,f) retained some semblance of open porosity at all three loadings, whereas curcumin impregnation (Figure 2g–f) led to total blockage of the MOF structure above 30 wt % loading. Such effects demonstrate that the larger curcuminoids lead to more filling of both the MOF pore and the crystalline surface, whereas the smaller species preferentially filled the micropores without blocking the particle faces, themselves. Indeed, the textural properties summarized in Table 2 corroborated these findings, given that the curcumin-

Table 2. Textural Properties of the Bare Mg-74-MOF and the Drug-Loaded MOF Samples

sample	drug loading (wt %)	S_{BET} (m^2/g)	V_{micro} (cm^3/g)	V_{meso} (cm^3/g)	d_p (nm)
Mg-MOF-74	0	950	0.31	0.08	2, 13
MOF-Ibu-30	30	30	0	0.07	3, 4.9, 9, 13
MOF-Ibu-50	50	10	0	0.03	3, 4.9, 9.1, 13
MOF-Ibu-80	80	10	0	0.02	2.9, 4.9, 9.1, 13, 22
MOF-Flu-30	30	30	0	0.06	2.9, 3.7, 4.7, 8.2, 13
MOF-Flu-50	50	30	0	0.05	3, 5.1, 9, 14, 21
MOF-Flu-80	80	10	0	0.03	3, 4.9, 7.9, 14
MOF-Cur-30	30	20	0	0.03	3.1, 5.2, 9.5, 13.2
MOF-Cur-50	50	15	0	0.01	3.2, 4.7, 12.5
MOF-Cur-80	80	10	0	0.01	

loaded MOF became mostly nonporous even at 30 wt % drug loading. Similar effects were shown in our previous works and were somewhat expected given the differences in molecular sizes and solubilities of these drugs.^{8,15,24,25} In the context of how these differences in the drug loading mechanism would be expected to influence pharmacokinetic release rates, without even considering solubility, one would anticipate that curcumin would have the worst rates of diffusivity. The reason being that such total blockage of the MOF crystalline faces would render the Mg clusters to be less soluble, thereby causing the release profile to be mostly driven by the rate of single-layer effusion of the drug film.^{8,15,24,25} Given the large molecular size of curcuminoids coupled with their poor solubility in PBS, such a rate would be expected to be quite slow.¹⁸

To assess any changes in the crystallinity of Mg-MOF-74 after encapsulation of ibuprofen, 5-fluorouracil, and curcumin, XRD analysis was run on the bare MOF and drug-loaded samples, and the corresponding spectra are presented in Figure 3. As evident from these spectra, all the samples displayed several major peaks at 6.8, 11.8, and 18.2°, which were related to (110), (300), and (410) diffractive indices, respectively.^{33–35} It should be noted that these planes were all retained in the ibuprofen- (Figure 3b), 5-fluorouracil- (Figure 3c), and curcumin-impregnated (Figure 3d) composites, once again indicating that Mg MOF-74 can undergo drug impregnation without degrading its crystalline structure.²⁶ However, it should be noted that the curcumin-impregnated

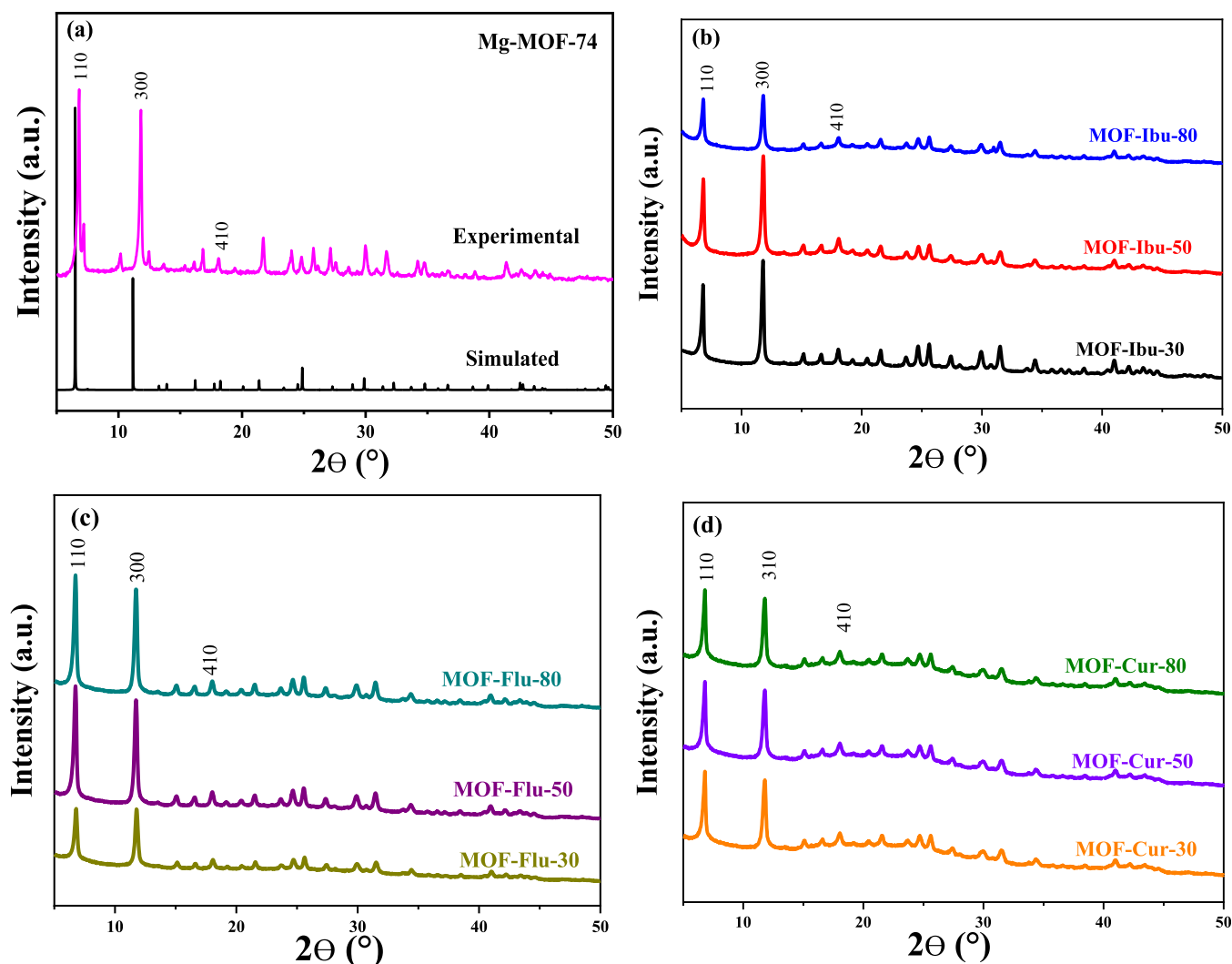


Figure 3. XRD patterns for (a) bare Mg-MOF-74, (b) ibuprofen-loaded Mg-MOF-74, (c) 5-fluorouracil-loaded Mg-MO-74, and (d) curcumin-loaded Mg-MOF-74.

samples did show more signs of amorphism—particularly between $2\theta = 15\text{--}35^\circ$ —which further supported that the larger drug was deposited on the MOF crystalline faces. These findings are consistent with the N_2 physisorption data in Figure 2, which suggest that curcumin fully covered the MOF particles. Such qualitative results further suggested that the release rate of curcumin would likely be the slowest, although the release rate mechanisms of ibuprofen or fluorouracil could not be predicted purely from the characterizations alone.

3.2. Drug Release Experiments. The raw drug release concentration profiles were quantified for the three samples from 30 to 80 wt % across 24 h by HPLC, as shown in Figure 4. Evidently, the amount of drug delivered increased by an amount consistent with the weight loading. It should be noted here that the three drug release concentrations should not be compared to one another by their raw quantities, given that the detection intensity will vary across compounds, which skews direct comparison of ibuprofen/curcumin/5-fluorouracil concentrations from the raw HPLC-integrated quantifications. It is thusly more useful to compare the concentration profiles in the context of singular drugs at three loadings. In this regard, it should be noted that the ibuprofen and curcumin profiles (Figure 4a,c) showed nearly single-release pharmacokinetic

fronts, whereas two-step releases were observed for 5-fluorouracil (Figure 4b). These release mechanisms corresponded with the previous characterizations, namely, in that 5-fluorouracil was released stepwise from the MOF surface, whereas ibuprofen and curcumin showed quantifiable release from the MOF pore, followed by rapid release from the microparticulate after Mg dissolution.⁸ This effect was more clearly pronounced in the ibuprofen samples, which may signify some semblance of weaker MOF/drug interaction as compared to 5-fluorouracil. The underlying mechanism being that ibuprofen was more readily extracted from the MOF without dissolving the crystalline structure, whereas 5-fluorouracil extraction occurred more favorably when the MOF started to decompose around $t = 3$ h. This result was somewhat surprising given that 5-fluorouracil is more soluble than ibuprofen; hence, it likely was caused by some differences in noncovalent electrostatic bonding. Nevertheless, more investigations are required to better understand the exact mechanism of release for each drug and to determine the rate-limiting step in releasing drugs from Mg-MOF-74.

To gain a better understanding of the relationship between drug characteristics and pharmacokinetic performance of the MOF nanocarrier, the raw drug concentrations determined

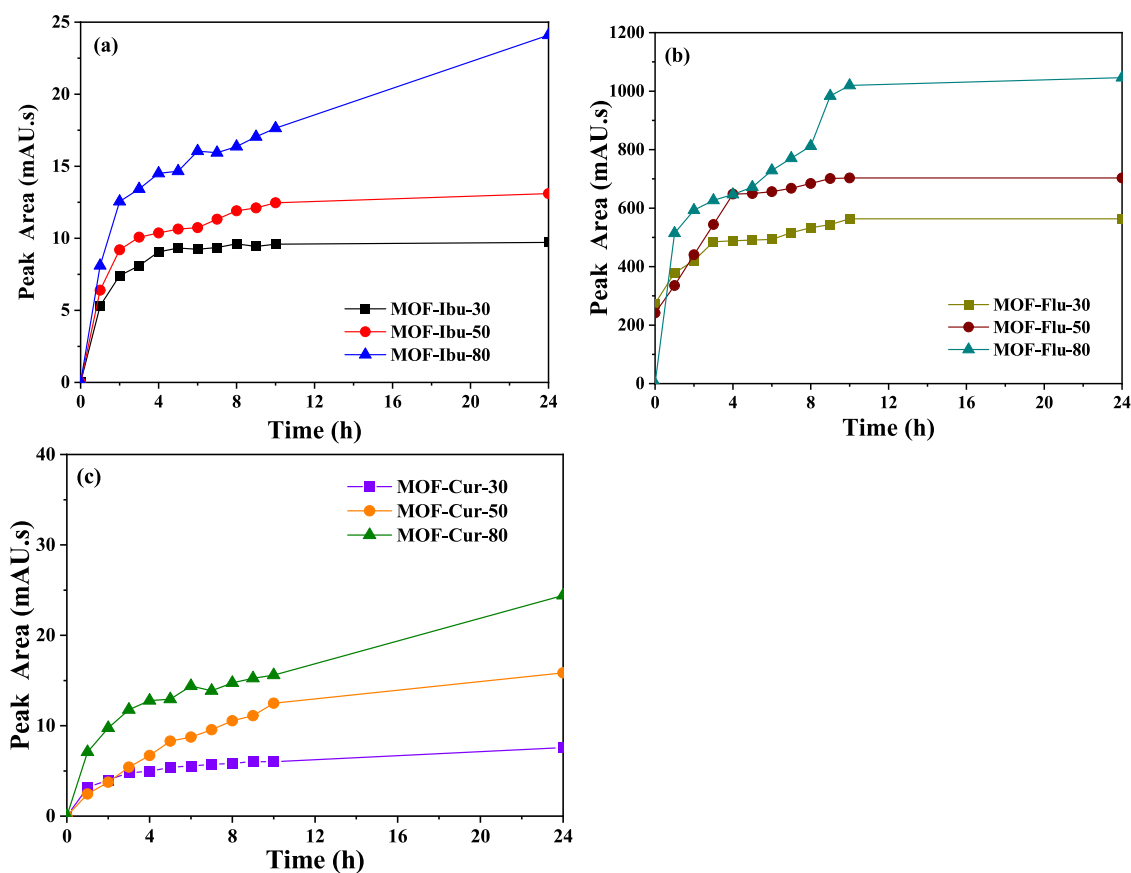


Figure 4. Peak concentration profiles from HPLC experiments for (a) ibuprofen-loaded Mg-MOF-74, (b) 5-fluorouracil-loaded Mg-MOF-74, and (c) curcumin-loaded Mg-MOF-74 in PBS at 37 °C.

from HPLC experiments were normalized, and the resulting delivery profiles were fitted with the Higuchi model.^{10,15} The pharmacokinetic profiles are presented in Figure 5, while the estimated release rate constants (k) are listed in Table 2 for all samples studied. Looking at the normalized release rate profiles, the maximum C/C_0 value was achieved by MOF-Flu-30, which was 98% after 10 h of release time, whereas the least amount released was 59%, which was displayed by MOF-Cur-80. After 1 h of exposure to PBS, 82% of the drug was released from MOF-Flu-30, which was 1.9 and 2.7 times higher than those released from MOF-Ibu-30 and MOF-Cur-30, respectively. Given the similar surface area and pore volume of the drug-loaded samples at fixed loadings, these drug release results could be directly correlated with the degree of the solubility of the pharmaceutical species, as stated earlier.

Moreover, it should be noted that all the R^2 had a value greater than 88%, implying that the Higuchi model was relatively a suitable model to fit the drug delivery data within the first 10 h of release. This was also indicated that the diffusion of the drugs through the pores of Mg-MOF-74 is the primary mechanism controlling the release rate and overall transport of the species from the MOF to the PBS solution during the first phase of delivery, and not by layered release from the MOF surface.^{36,37} From the data presented in Table 3, it was apparent that the pharmacokinetic constants were a strong function of drug loading in all the three cases, showing a decreasing trend with drug loading. The saturation of the MOF pores with the drug at higher loadings leads to diffusion resistances within the material during the release, which adversely affects the pharmacokinetics. Such diffusion pore

resistance is clearly reflected on the k values reported here. Across the three drugs, the release rate constant was the highest for the 5-fluorouracil drug compared to the ibuprofen and curcumin at fixed drug loadings. The highest k value was found to be $0.34 \text{ h}^{-1/2}$ for MOF-Flu-30 and the lowest for MOF-Cur-80 at $0.18 \text{ h}^{-1/2}$. These values are comparable to the literature data. For instance, k values of 0.21 and $0.11 \text{ h}^{-1/2}$ were reported for 25.5 wt % ibuprofen loaded on MIL-100 (Fe) and UiO-66, respectively.³⁸ As noted in Table 1, 5-fluorouracil has the highest solubility in PBS among the three drugs, while also being less bulky. The combination of these factors can contribute to fastest release kinetics from the MOF upon exposure to the PBS solution for this drug even though its molecular weight is the highest. It is also noted that the release constants follow the loading amounts for all the three drugs and show a decreasing trend upon increasing the incorporated amount. The results confirm the dependency of pharmacokinetic behavior of Mg-MOF-74 on the concentration, solubility, and type of the drug loaded; nevertheless, given that these pharmacokinetic rates are comparable to the reported data in the literature, this MOF can be concluded to be a suitable drug carrier for a wide variety of the drugs.

4. CONCLUSIONS

In this study, we investigated the pharmacokinetic behavior of Mg-MOF-74 for effective release of three model drugs, namely, ibuprofen, 5-fluorouracil, and curcumin, with varied drug loading. This nanocarrier was impregnated with 30, 50, and 80 wt % of these three drugs and studied in drug release experiments. The characterization results confirmed successful

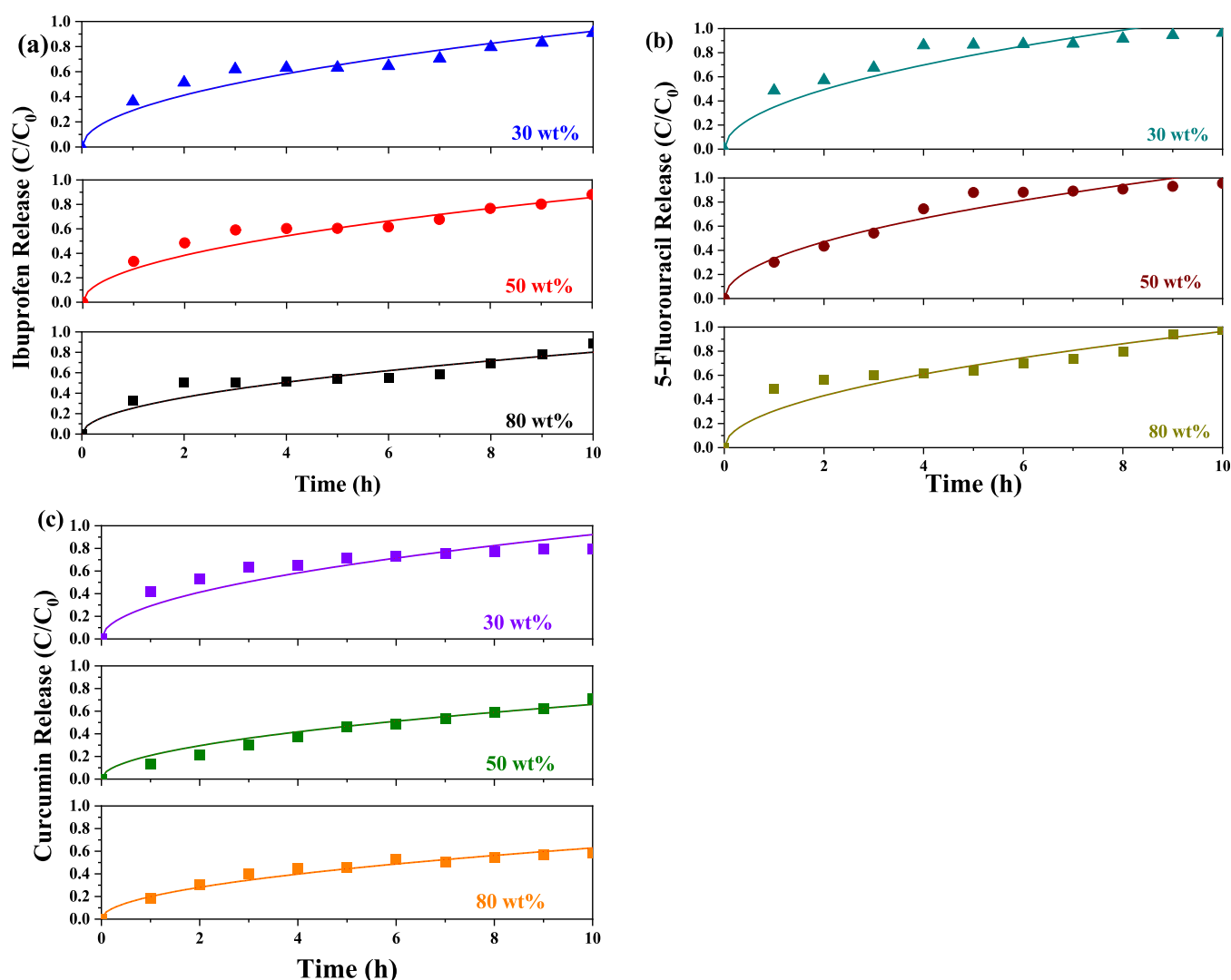


Figure 5. Normalized concentration profiles with Higuchi technique curve fittings for (a) ibuprofen-loaded Mg-MOF-74, (b) 5-fluorouracil-loaded Mg-MO-74, and (c) curcumin-loaded Mg-MOF-74.

Table 3. Calculated Release Rate Constants from Drug Delivery Experiments for Ibuprofen, 5-Fluorouracil, and Curcumin from Mg-MOF-74

adsorbent	release rate constant ($\text{h}^{-1/2}$)	R^2
MOF-Ibu-30	0.29	0.94
MOF-Ibu-50	0.27	0.95
MOF-Ibu-80	0.25	0.95
MOF-Flu-30	0.34	0.89
MOF-Flu-50	0.32	0.95
MOF-Flu-80	0.30	0.89
MOF-Cur-30	0.29	0.88
MOF-Cur-50	0.20	0.96
MOF-Cur-80	0.18	0.95

incorporation of the drugs within the MOF. The surface area and pore volume of Mg-MOF-74 decreased drastically as the amount of the impregnated drugs increased, and at 80 wt % loadings, the MOF completely lost its microporosity. Our drug release experiments indicated that at fixed drug loading, the release amount was the highest for 5-fluorouracil. By contrast, the release rate of curcumin was found to be the lowest compared to 5-fluorouracil and ibuprofen analogues. More-

over, for all the three drugs, the drug release constant exhibited a decreasing trend with drug loading. Overall, the findings of this study confirm the potential of biocompatible Mg-MOF74 as a great drug carrier candidate for ibuprofen, 5-fluorouracil, and curcumin.

AUTHOR INFORMATION

Corresponding Author

Fateme Rezaei – Linda and Bipin Doshi Department of Chemical and Biochemical Engineering, Missouri University of Science and Technology, Rolla, Missouri 65409-1230, United States; orcid.org/0000-0002-4214-4235; Email: rezaeif@mst.edu

Authors

Neila Pederneira – Linda and Bipin Doshi Department of Chemical and Biochemical Engineering, Missouri University of Science and Technology, Rolla, Missouri 65409-1230, United States

Kyle Newport – Linda and Bipin Doshi Department of Chemical and Biochemical Engineering, Missouri University of Science and Technology, Rolla, Missouri 65409-1230, United States

Shane Lawson – Linda and Bipin Doshi Department of Chemical and Biochemical Engineering, Missouri University of Science and Technology, Rolla, Missouri 65409-1230, United States

Ali A. Rownaghi – Department of Chemistry, Cleveland State University, Cleveland, Ohio 44115, United States;

orcid.org/0000-0001-5228-5624

Complete contact information is available at:
<https://pubs.acs.org/10.1021/acsabm.3c00275>

Notes

The authors declare no competing financial interest.

ACKNOWLEDGMENTS

The authors acknowledge the Materials Research Center (MRC) at the Missouri University of Science and Technology for conducting the XRD characterizations. The involvement of AR in this work was sponsored by the National Science Foundation (NSF CBET-2019350).

REFERENCES

- (1) Lawson, H. D.; Walton, S. P.; Chan, C. Metal-Organic Frameworks for Drug Delivery: A Design Perspective. *ACS Appl. Mater. Interfaces* **2021**, *13*, 7004–7020.
- (2) He, S.; Wu, L.; Li, X.; Sun, H.; Xiong, T.; Liu, J.; Huang, C.; Xu, H.; Sun, H.; Chen, W.; Gref, R.; Zhang, J. Metal-Organic Frameworks for Advanced Drug Delivery. *Acta Pharm. Sin. B* **2021**, *11*, 2362–2395.
- (3) Alqahtani, M. S.; Kazi, M.; Alsenaidy, M. A.; Ahmad, M. Z. Advances in Oral Drug Delivery. *Front. Pharmacol.* **2021**, *12*, 618411.
- (4) Varrassi, G.; Pergolizzi, J. V.; Dowling, P.; Paladini, A. Ibuprofen Safety at the Golden Anniversary: Are All NSAIDs the Same? A Narrative Review. *Adv. Ther.* **2020**, *37*, 61–82.
- (5) Lucena, F. R. S.; de Araújo, L. C. C.; do D. Rodrigues, M.; da Silva, T. G.; Pereira, V. R. A.; Militão, G. C. G.; Fontes, D. A. F.; Rolim-Neto, P. J.; da Silva, F. F.; Nascimento, S. C. Induction of Cancer Cell Death by Apoptosis and Slow Release of 5-Fluoracil from Metal-Organic Frameworks Cu-BTC. *Biomed. Pharmacother.* **2013**, *67*, 707–713.
- (6) Horcajada, P.; Chalati, T.; Serre, C.; Gillet, B.; Sebrie, C.; Baati, T.; Eubank, J. F.; Heurtaux, D.; Clayette, P.; Kreuz, C.; Chang, J. S.; Hwang, Y. K.; Marsaud, V.; Bories, P. N.; Cynober, L.; Gil, S.; Férey, G.; Couvreur, P.; Gref, R. Porous Metal-Organic-Framework Nanoscale Carriers as a Potential Platform for Drug Delivery and Imaging. *Nat. Mater.* **2010**, *9*, 172–178.
- (7) Grant Glover, T.; Peterson, G. W.; Schindler, B. J.; Britt, D.; Yaghi, O. MOF-74 Building Unit Has a Direct Impact on Toxic Gas Adsorption. *Chem. Eng. Sci.* **2011**, *66*, 163–170.
- (8) Lawson, S.; Newport, K.; Pederniera, N.; Rownaghi, A. A.; Rezaei, F. Curcumin Delivery on Metal-Organic Frameworks: The Effect of the Metal Center on Pharmacokinetics within the M-MOF-74 Family. *ACS Appl. Bio Mater.* **2021**, *4*, 3423–3432.
- (9) Hartlieb, K. J.; Ferris, D. P.; Holcroft, J. M.; Kandela, I.; Stern, C. L.; Nassar, M. S.; Botros, Y. Y.; Stoddart, J. F. Encapsulation of Ibuprofen in CD-MOF and Related Bioavailability Studies. *Mol. Pharm.* **2017**, *14*, 1831–1839.
- (10) Liu, X.; Wang, Y.; Yuan, J.; Li, X.; Wu, S.; Bao, Y.; Feng, Z.; Ou, F.; He, Y. Prediction of the Ibuprofen Loading Capacity of MOFs by Machine Learning. *Bioengineering* **2022**, *9*, 517.
- (11) Suwardi, A.; Wang, F. K.; Xue, K.; Han, M. Y.; Teo, P.; Wang, P.; Wang, S.; Liu, Y.; Ye, E.; Li, Z.; Loh, X. J. Machine Learning-Driven Biomaterials Evolution. *Adv. Mater.* **2022**, *34*, 2102703.
- (12) Wang, Y.; Yan, J.; Wen, N.; Xiong, H.; Cai, S.; He, Q.; Hu, Y.; Peng, D.; Liu, Z.; Liu, Y. Metal-Organic Frameworks for Stimuli-Responsive Drug Delivery. *Biomaterials* **2020**, *230*, 119619.
- (13) Wu, M. X.; Yang, Y. W. Metal–Organic Framework (MOF)-Based Drug/Cargo Delivery and Cancer Therapy. *Adv. Mater.* **2017**, *29*, 1606134.
- (14) Ashrafizadeh, M.; Hushmandi, K.; Rahmani Moghadam, E.; Zarrin, V.; Hosseinzadeh Kashani, S.; Bokaie, S.; Najafi, M.; Tavakol, S.; Mohammadinejad, R.; Nabavi, N.; Hsieh, C. L.; Zarepour, A.; Zare, E. N.; Zarrabi, A.; Makvandi, P. Progress in Delivery of siRNA-Based Therapeutics Employing Nano-Vehicles for Treatment of Prostate Cancer. *Bioengineering* **2020**, *7*, 91.
- (15) Lawson, S.; Newport, K.; Schueddig, K.; Rownaghi, A. A.; Rezaei, F. Optimizing Ibuprofen Concentration for Rapid Pharmacokinetics on Biocompatible Zinc-Based MOF-74 and UTSA-74. *Mater. Sci. Eng., C* **2020**, *117*, 111336.
- (16) Thakkar, A.; Chenreddy, S.; Wang, J.; Prabhu, S. Evaluation of Ibuprofen Loaded Solid Lipid Nanoparticles and Its Combination Regimens for Pancreatic Cancer Chemoprevention. *Int. J. Oncol.* **2015**, *46*, 1827–1834.
- (17) Patel, G.; Yadav, B. K. Formulation, Characterization and In Vitro Cytotoxicity of 5-Fluorouracil Loaded Polymeric Electrospun Nanofibers for the Treatment of Skin Cancer. *Recent Pat. Nanotechnol.* **2019**, *13*, 114–128.
- (18) Yallapu, M. M.; Jaggi, M.; Chauhan, S. C. Curcumin nanomedicine: a road to cancer therapeutics. *Curr. Pharm. Des.* **2013**, *19*, 1994–2010.
- (19) Wang, H. L.; Yeh, H.; Li, B. H.; Lin, C. H.; Hsiao, T. C.; Tsai, D. H. Zirconium-Based Metal-Organic Framework Nanocarrier for the Controlled Release of Ibuprofen. *ACS Appl. Nano Mater.* **2019**, *2*, 3329–3334.
- (20) Orellana-Tavra, C.; Marshall, R. J.; Baxter, E. F.; Lázaro, I. A.; Tao, A.; Cheetham, A. K.; Forgan, R. S.; Fairen-Jimenez, D. Drug Delivery and Controlled Release from Biocompatible Metal-Organic Frameworks Using Mechanical Amorphization. *J. Mater. Chem. B* **2016**, *4*, 7697–7707.
- (21) Souza, B. E.; Donà, L.; Titov, K.; Bruzzese, P.; Zeng, Z.; Zhang, Y.; Babal, A. S.; Möslin, A. F.; Frogley, M. D.; Wolna, M.; Cinque, G.; Civalleri, B.; Tan, J. C. Elucidating the Drug Release from Metal-Organic Framework Nanocomposites via in Situ Synchrotron Microspectroscopy and Theoretical Modeling. *ACS Appl. Mater. Interfaces* **2020**, *12*, 5147–5156.
- (22) Huxford, R. C.; Della Rocca, J.; Lin, W. Metal-Organic Frameworks as Potential Drug Carriers. *Curr. Opin. Chem. Biol.* **2010**, *14*, 262–268.
- (23) Wu, X.; Bao, Z.; Yuan, B.; Wang, J.; Sun, Y.; Luo, H.; Deng, S. Microwave Synthesis and Characterization of MOF-74 (M = Ni, Mg) for Gas Separation. *Microporous Mesoporous Mater.* **2013**, *180*, 114–122.
- (24) Lawson, S.; Rownaghi, A. A.; Rezaei, F. Combined Ibuprofen and Curcumin Delivery Using Mg-MOF-74 as a Single Nanocarrier. *ACS Appl. Bio Mater.* **2022**, *5*, 265–271.
- (25) Lawson, S.; Siemers, A.; Kostlenick, J.; Al-Naddaf, Q.; Newport, K.; Rownaghi, A. A.; Rezaei, F. Mixing Mg-MOF-74 with Zn-MOF-74: A Facile Pathway of Controlling the Pharmacokinetic Release Rate of Curcumin. *ACS Appl. Bio Mater.* **2021**, *4*, 6874–6880.
- (26) Fonseca-Santos, B.; Gremião, M. P. D.; Chorilli, M. A Simple Reversed Phase High-Performance Liquid Chromatography (HPLC) Method for Determination of in Situ Gelling Curcumin-Loaded Liquid Crystals in in Vitro Performance Tests. *Arab. J. Chem.* **2017**, *10*, 1029–1037.
- (27) Doadrio, A.; Sousa, E.; Doadrio, J.; Pérez Pariente, J.; Izquierdo-Barba, I.; Vallet-Regí, M. Mesoporous SBA-15 HPLC Evaluation for Controlled Gentamicin Drug Delivery. *J. Controlled Release* **2004**, *97*, 125–132.
- (28) Higuchi, T. Mechanism of sustained-action medication. Theoretical analysis of rate of release of solid drugs dispersed in solid matrices. *J. Pharm. Sci.* **1963**, *52*, 1145–1149.
- (29) Paarakh, M. P.; Jose, P. A.; Setty, C. M.; Christopher, G. V. P. Release kinetics—Concepts and applications. *Int. J. Pharm. Technol.* **2019**, *8*, 12–20.

(30) Mohan, P. K.; Sreelakshmi, G.; Muraleedharan, C. V.; Joseph, R. Water Soluble Complexes of Curcumin with Cyclodextrins: Characterization by FT-Raman Spectroscopy. *Vib. Spectrosc.* **2012**, *62*, 77–84.

(31) Gangwar, R. K.; Dhumale, V. A.; Kumari, D.; Nakate, U. T.; Gosavi, S. W.; Sharma, R. B.; Kale, S. N.; Datar, S. Conjugation of Curcumin with PVP Capped Gold Nanoparticles for Improving Bioavailability. *Mater. Sci. Eng., C* **2012**, *32*, 2659–2663.

(32) Thommes, M.; Kaneko, K.; Neimark, A. V.; Olivier, J. P.; Rodriguez-Reinoso, F.; Rouquerol, J.; Sing, K. S. W. Physisorption of Gases, with Special Reference to the Evaluation of Surface Area and Pore Size Distribution (IUPAC Technical Report). *Pure Appl. Chem.* **2015**, *87*, 1051–1069.

(33) Rezaei, F.; Lawson, S.; Hosseini, H.; Thakkar, H.; Hajari, A.; Monjezi, S.; Rownaghi, A. A. MOF-74 and UTSA-16 Film Growth on Monolithic Structures and Their CO₂ Adsorption Performance. *Chem. Eng. J.* **2017**, *313*, 1346–1353.

(34) Lawson, S.; Hajari, A.; Rownaghi, A. A.; Rezaei, F. MOF Immobilization on the Surface of Polymer-Cordierite Composite Monoliths through in-Situ Crystal Growth. *Sep. Purif. Technol.* **2017**, *183*, 173–180.

(35) Pu, S.; Wang, J.; Li, L.; Zhang, Z.; Bao, Z.; Yang, Q.; Yang, Y.; Xing, H.; Ren, Q. Performance Comparison of Metal-Organic Framework Extrudates and Commercial Zeolite for Ethylene/Ethane Separation. *Ind. Eng. Chem. Res.* **2018**, *57*, 1645–1654.

(36) Saravanan, M.; Bhaskar, K.; Rao, G. S.; Dhanaraju, M. D. Ibuprofen-Loaded Ethylcellulose/Polystyrene Microspheres: An Approach to Get Prolonged Drug Release with Reduced Burst Effect and Low Ethylcellulose Content. *J. Microencapsul.* **2003**, *20*, 289–302.

(37) Latifi, L.; Sohrabnezhad, S. Drug Delivery by Micro and Meso Metal-Organic Frameworks. *Polyhedron* **2020**, *180*, 114321.

(38) Rojas, S.; Colinet, I.; Cunha, D.; Hidalgo, T.; Salles, F.; Serre, C.; Guillou, N.; Horcajada, P. Toward Understanding Drug Incorporation and Delivery from Biocompatible Metal-Organic Frameworks in View of Cutaneous Administration. *ACS Omega* **2018**, *3*, 2994–3003.

Recommended by ACS

Drug-Facilitated Crystallization of Spray-Dried CD-MOFs with Tunable Morphology, Porosity, And Dissolution Profile

Kazunori Kadota, Shunsuke Tanaka, *et al.*

MAY 15, 2023
ACS APPLIED BIO MATERIALS

READ 

Engineering the Morphostructural Properties and Drug Loading Degree of Organic–Inorganic Fluorouracil–MgAl LDH Nanohybrids by Rational Control of Hydrothermal...

Alina Ibanescu, Brindusa Dragoi, *et al.*

JULY 12, 2023
ACS OMEGA

READ 

Fabrication of Porous Fe-Based Metal–Organic Complex for the Enhanced Delivery of 5-Fluorouracil in In Vitro Treatment of Cancer Cells

Bac Thanh Le, Duong Duc La, *et al.*

DECEMBER 09, 2022
ACS OMEGA

READ 

Synthesis and Application of MOF-808 Decorated with Folic Acid-Conjugated Chitosan as a Strong Nanocarrier for the Targeted Drug Delivery of Quercetin

Mozhgan Parsaei and Kamran Akhbari

NOVEMBER 16, 2022
INORGANIC CHEMISTRY

READ 

Get More Suggestions >